

A New Type of Cesium-ion-conducting Solid

Shinji Tamura, Taku Nishikawa, and Nobuhito Imanaka*

Department of Applied Chemistry, Faculty of Engineering, Osaka University, 2-1 Yamadaoka, Suita, Osaka 565-0871

(Received October 27, 2010; CL-100913; E-mail: imanaka@chem.eng.osaka-u.ac.jp)

High Cs⁺ ion conductivity was successfully realized in solids at temperatures below 250 °C by doping Cs-bis(trifluoromethanesulfonyl) amide (CsTFSA) into cubic rare earth oxides of R₂O₃. Among the (1 - x)R₂O₃-xCsTFSA solids prepared, a 0.75Gd₂O₃-0.25CsTFSA solid showed the highest Cs⁺ ion conductivity of 3.4 × 10⁻² S cm⁻¹ at 250 °C, which is the highest value yet reported for a solid Cs⁺ ion conductor.

Solid electrolytes are functional materials in which a single ionic species macroscopically migrates through the solid to carry an electric current and are in demand for use in various types of electronic devices such as rechargeable batteries and chemical sensors. It is generally accepted that in solid electrolytes, ion conduction greatly depends upon the valence state of the conducting ion and that lower valence cations can migrate more easily than higher valence cations due to their weaker electrostatic interaction with the surrounding counter ions. Therefore, various solid electrolytes in which the conducting ions are monovalent cations such as Li⁺, Na⁺, K⁺, Ag⁺, and Cu⁺ have been extensively studied as fast ion conductors. However, ionic conduction in solids is also influenced by the size of the conducting ion. As a result, high ionic conductivities have been obtained using smaller cations like Li⁺ (ionic radius: 0.076 nm [coordination number (CN): 6]¹) and Na⁺ (0.102 nm [CN: 6]¹), because these smaller cations can smoothly migrate even in a rigid crystal lattice. Although the larger Cs⁺ ion (0.167 nm [CN: 6]¹) has been reported to conduct in solids such as Cs-β-ferrite,² Cs_{3-4x}M_xPO₄ (M = Zr, Hf, or Ce),³ and M'₂O₃-TiO₂-Cs₂O (M' = Ga or Fe),^{4,5} the use of these solids is problematic; Cs⁺-β-ferrite is a mixed conductor with Cs⁺ and electron conduction, and both Cs_{3-4x}M_xPO₄ and M'₂O₃-TiO₂-Cs₂O solids have low ionic conductivities at low temperatures (<10⁻³ S cm⁻¹ at 300 °C). A solid electrolyte with a highly pure Cs⁺ ion conductivity at temperatures below 300 °C has not yet been realized.

Recently, we have successfully developed a new type of ion-conducting solid, (1 - x)R₂O₃-xKNO₃ (R = Gd or Gd_{0.4}Nd_{0.6}),⁶⁻⁸ in which the conducting cation is the large K⁺ ion (0.138 nm [CN: 6]¹), by doping KNO₃ into cubic rare earth oxides of R₂O₃. These solids showed an extraordinarily high K⁺ ion conductivity above the melting point of KNO₃, which is comparable to those of Li⁺ and Na⁺ conductors. Furthermore, the temperature range for high K⁺ ion conductivity was lowered by doping with a potassium salt with a low melting point. Since the doping of an alkali metal salt into a cubic rare earth oxide in which large open spaces exist in the crystal lattice is an effective method of realizing high ionic conductivity for a large cation such as K⁺ even at low temperatures (<300 °C), it is expected that this technique can also be applied to Cs⁺ ion conduction in solids.

In this study, in order to develop a Cs⁺-ion-conducting solid with high conductivity at temperatures below 300 °C, we doped

a cesium salt, Cs-bis(trifluoromethanesulfonyl) amide (Cs(CF₃-SO₂)₂N: CsTFSA) (mp 126 °C) into R₂O₃ and investigated the Cs⁺ ion conductivity of the resulting (1 - x)R₂O₃-xCsTFSA solids. Because only heavy rare earth (Gd-Lu, Y, and Sc) oxides can have a cubic structure, we selected Gd₂O₃, Y₂O₃, and Lu₂O₃ as representative of cubic R₂O₃ but with different lattice sizes in order to investigate the effect of the lattice size on the Cs⁺ ion conductivity.

CsTFSA was prepared in an Ar atmosphere. After mixing Cs₂CO₃ with HTFSA in ethanol at 80 °C for 12 h, the desired CsTFSA solid was obtained by vaporizing ethanol at 90 °C. The (1 - x)R₂O₃-xCsTFSA solids were obtained by mixing R₂O₃ (R = Gd, Y, or Lu) and CsTFSA in an agate mortar and then heating at 250 °C for 12 h in a synthetic air atmosphere.

The samples prepared were identified by X-ray powder diffraction (XRD) measurements (MultiFlex, Rigaku) with Cu Kα radiation in a 2θ range of 10–70° with a step width of 0.04° at room temperature. The lattice parameters of the samples were precisely determined by an internal standard method using α-Al₂O₃. The decomposition temperatures of the samples were investigated by differential thermal analysis (DTA; DTG-50H, Shimadzu) with a flow of synthetic air.

The ac conductivity of sample pellets sintered at 250 °C for 12 h was measured by complex impedance (HP4192A, Hewlett Packard) in the frequency range of 5–13 MHz. Before these measurements, sputter-deposited Au film electrodes were prepared in the centers of the top and bottom surfaces of the pellet. The conducting species in 0.75Gd₂O₃-0.25CsTFSA was investigated by polarization measurements in various atmospheres and by dc electrolysis in atmospheric air. The polarization behavior was studied by estimating the dc to ac conductivity ratio (σ_{dc}/σ_{ac}), where σ_{dc} was calculated from the dc voltage generated when a constant dc current of 1 μA was passed through the sintered sample pellet. DC electrolysis was carried out by applying a dc voltage of 4 V to a sample pellet sandwiched by Au bulk electrodes at 200 °C for 48 h. After the dc electrolysis, the area of the electrolyzed sample surface that had been in contact with the Au electrode was investigated by XRD. Furthermore, the elemental distribution in the electrolyzed sample was examined by electron probe microanalysis (EPMA; EPMA-1500, Shimadzu).

XRD measurements of (1 - x)Gd₂O₃-xCsTFSA solids calcined at 250 °C for 12 h in an air atmosphere (Figure S1 in the Supporting Information)⁹ indicated that a single-phase cubic rare earth oxide structure was obtained for samples with x ≤ 0.25, while samples with x > 0.25 were a two-phase mixture of cubic Gd₂O₃ and CsTFSA. For samples of R = Y and Lu (Figures S2 and S3),⁹ similar XRD patterns to the samples of R = Gd were obtained; the compositional region of single-phase cubic R₂O₃ was x ≤ 0.15 for R = Y and x ≤ 0.10 for R = Lu. Figure 1 presents the compositional dependencies of the lattice volume of the cubic R₂O₃ phase in the prepared

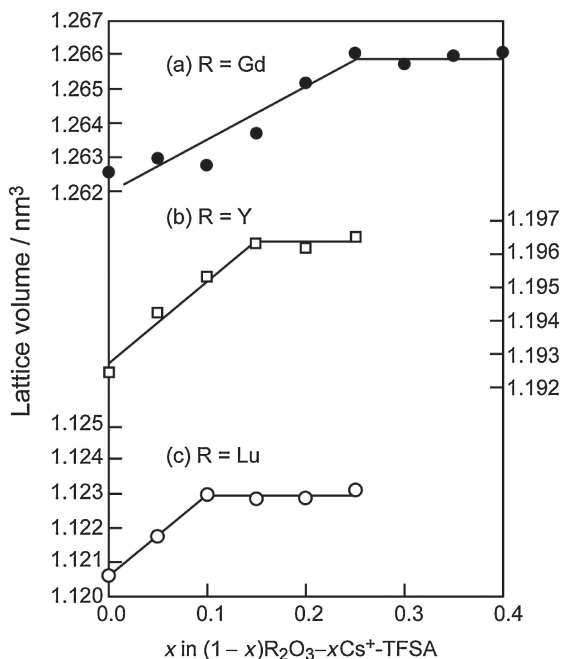


Figure 1. Compositional dependence of the lattice volume of the cubic R_2O_3 phase of $(1-x)R_2O_3-xCsTFSA$ ($R = Gd$ (a), Y (b), and Lu (c)) solids.

samples of $(1-x)R_2O_3-xCsTFSA$ ($R = Gd, Y, \text{ or } Lu$) solids. For each series, the lattice volume of the R_2O_3 phase increased linearly with increasing $CsTFSA$ doping within the composition range of the single-phase R_2O_3 structure ($x = 0.25$ ($R = Gd$), 0.15 ($R = Y$), and 0.10 ($R = Lu$)). The lattice volume was constant for samples containing amounts of $CsTFSA$ above this composition limit. Furthermore, we have confirmed the existence of $CsTFSA$ in the samples sintered at $250^\circ C$ by TG-DTA analysis (Figure S4).⁹ These results indicate that the $CsTFSA$ was successfully doped into the mother cubic R_2O_3 structure, forming an interstitial solid solution, in which Cs^+ ions partially replaced R^{3+} sites. In this situation, charge compensation would be realized by the existence of $TFSA^-$ anions in the grain boundary.

In order to confirm the solid solubility of $CsTFSA$ in R_2O_3 , we measured the electrical conductivity of $0.9R_2O_3-0.1CsTFSA$ ($R = Gd, Y, \text{ or } Lu$) solids at $250^\circ C$, for compositions within the solid solubility limit of each series. Figure 2 depicts the compositional dependencies of the electrical conductivity and the activation energy for Cs^+ ion conduction in the samples (Cs^+ ion conduction is demonstrated below). Based on the lattice volume of the samples, the Cs^+ ion conductivity increase accompanied a decrease in activation energy. This tendency is supported by the generally accepted idea that ionic migration in solids is strongly influenced by the size of the conducting pathway, which is directly related to the lattice volume for solids with the same crystal structure. Therefore, the $(1-x)R_2O_3-xCsTFSA$ ($x \leq 0.25$ ($R = Gd$), 0.15 ($R = Y$), and 0.10 ($R = Lu$)) solids clearly formed a solid solution.

To identify the conducting species (candidates were R^{3+} , Cs^+ , O^{2-} , and/or electronic (e^- and h^+) species), we investigated the dc to ac conductivity ratio (σ_{dc}/σ_{ac}) for a $0.75Gd_2O_3-0.25CsTFSA$ solid, which showed the highest conductivity of all

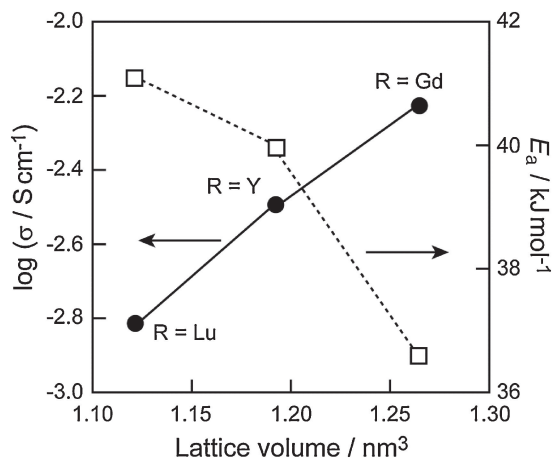


Figure 2. Lattice volume dependence of the electrical conductivity at $250^\circ C$ and the activation energy for Cs^+ ion conduction in $0.9R_2O_3-0.1CsTFSA$ ($R = Gd, Y, \text{ and } Lu$) solids.

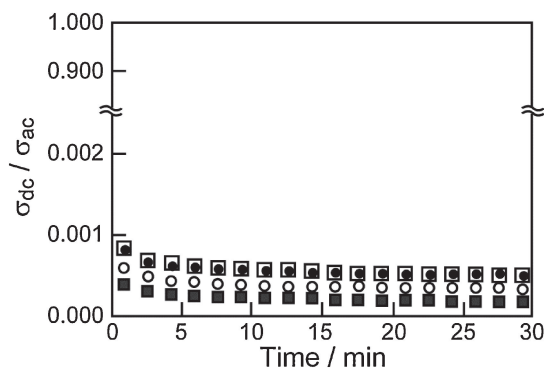


Figure 3. Time dependence of the dc to ac conductivity ratio (σ_{dc}/σ_{ac}) at $250^\circ C$ in O_2 (\square), He (\blacksquare), dry air (\circ), and wet air (\bullet) for a $0.75Gd_2O_3-0.25CsTFSA$ solid.

samples prepared (conductivity data for $(1-x)R_2O_3-xCsTFSA$ solids with compositions within the solid solubility limit are presented in Figure S5).⁹ Figure 3 shows the time dependence of the σ_{dc}/σ_{ac} ratio in O_2 , He , dry air, and wet air (H_2O : ca. 1 vol %) at $250^\circ C$. If the solid conducts O^{2-} ions, the dc conductivity in a high- P_{O_2} atmosphere should be high because the conducting O^{2-} ions are supplied to the sample from the atmosphere. As a result, the σ_{dc}/σ_{ac} ratio should be large in a high- P_{O_2} atmosphere. Similarly, for electronic conductors, the σ_{dc}/σ_{ac} ratio should always be high irrespective of P_{O_2} in ambient atmosphere. In other words, if the solid has an extraordinarily low σ_{dc}/σ_{ac} ratio in various atmospheres, the conducting species must be a cation. The σ_{dc}/σ_{ac} ratio in all atmospheres drastically decreased with time, reaching a value of less than 0.001, indicating that the conducting species in the $0.75Gd_2O_3-0.25CsTFSA$ solid is an R^{3+} or Cs^+ ion. Furthermore, the ionic transference number of the sample can be estimated from the equation, $t_{ion} = 1 - (\sigma_{dc}/\sigma_{ac})$, and was calculated to be above 0.999.

The conducting cation species in the $0.75Gd_2O_3-0.25CsTFSA$ solid was directly identified by dc electrolysis. Since the decomposition voltage of the sample was preliminarily determined to be ca. 1.2 V (This low decomposition voltage is

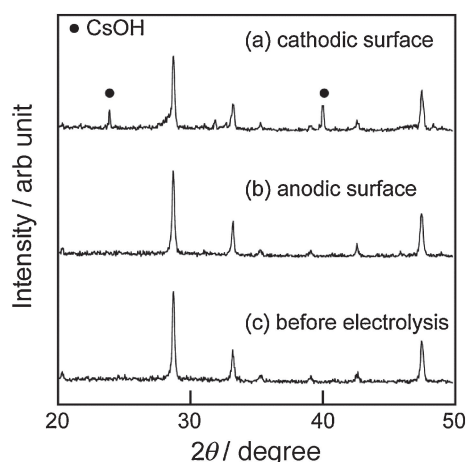
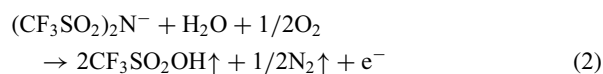
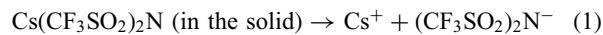


Figure 4. XRD patterns at the cathodic (a) and anodic surface (b) of an electrolyzed $0.75\text{Gd}_2\text{O}_3\text{-}0.25\text{CsTFSA}$ solid. The corresponding pattern of a sample before electrolysis is also shown (c).

thought to be caused by the decomposition of CsTFSA in the grain boundary of Gd_2O_3) from the $I\text{-}V$ relationship, we applied a dc voltage of 4 V to the sample to continuously produce the conducting ionic species within the sample. If the $0.75\text{Gd}_2\text{O}_3\text{-}0.25\text{CsTFSA}$ solid is a Cs^+ ion conductor, the following reactions would occur at the anodic and cathodic sides of the sample during electrolysis: Cs^+ ions would be generated at the anodic side by the applied dc voltage (eq 1) and would then migrate within the sample. After reaching the Cs^+ ions at the cathodic surface, where the Au bulk electrode was attached, Cs^+ ions would be reduced to the metallic state by electrons (eq 3). Since the dc electrolysis was carried out in atmospheric air containing O_2 ($P_{\text{O}_2} = 2.4 \times 10^4 \text{ Pa}$) and water vapor, there was no residue at the anodic side (eq 2). In addition, Cs_2O and/or CsOH should be observed only at the cathodic surface after reactions with O_2 and H_2O (eqs 4 and 5).

(anodic side)



(cathodic side)

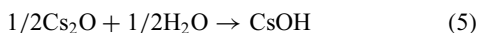
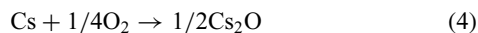
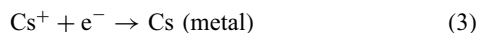


Figure 4 displays XRD patterns at the anodic and cathodic surfaces of an electrolyzed sample. CsOH was clearly observed at the cathodic surface of the electrolyzed sample pellet, although the XRD pattern at the anodic side was exactly the same as that of a sample before electrolysis. This strongly suggests that the above reactions did occur at the anodic and cathodic sides of the sample during electrolysis. Therefore, only Cs^+ ions migrated within the sample among the cationic species

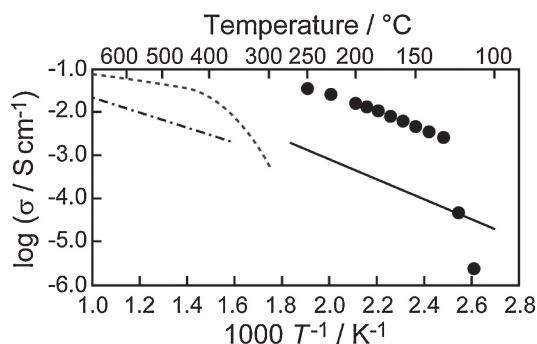


Figure 5. Temperature dependence of the Cs^+ ion conductivity of a $0.75\text{Gd}_2\text{O}_3\text{-}0.25\text{CsTFSA}$ solid (●) with the corresponding data for $\text{Cs-}\beta\text{-ferrite}$ (—),² $\text{Cs}_{2.9}\text{Ce}_{0.025}\text{PO}_4$ (- - -),³ and $0.95\text{Ga}_2\text{O}_3\text{-}0.05\text{TiO}_2\text{-Cs}_2\text{O}$ (- · -)⁴ solids.

in the sample. Although there is a possibility of the migration of TFSA^- anions in the grain boundary, in this case, the conductivity and the activation energy for conduction should be constant independent of the lattice volume. The results illustrated in Figure 2 suggest that the TFSA^- anion is not the conducting species in the present solid.

The temperature dependence of the Cs^+ ion conductivity for the $0.75\text{Gd}_2\text{O}_3\text{-}0.25\text{CsTFSA}$ solid is shown in Figure 5, along with the corresponding data for $\text{Cs-}\beta\text{-ferrite}$,² $\text{Cs}_{2.7}\text{Zr}_{0.075}\text{PO}_4$,³ and $0.95\text{Ga}_2\text{O}_3\text{-}0.05\text{TiO}_2\text{-Cs}_2\text{O}$ solids.⁴ Although the $\text{Cs}_{2.9}\text{-Ce}_{0.025}\text{PO}_4$ and $0.95\text{Ga}_2\text{O}_3\text{-}0.05\text{TiO}_2\text{-Cs}_2\text{O}$ solids, which have been reported to be Cs^+ ion conductors, showed a high electrical conductivity above 300°C , the extrapolated conductivities below 300°C are similar to that for $\text{Cs-}\beta\text{-ferrite}$. Furthermore, these solids exhibited some electronic conduction. On the other hand, the present $0.75\text{Gd}_2\text{O}_3\text{-}0.25\text{CsTFSA}$ solid, in which the predominant conducting species was a Cs^+ ion, exhibited a higher conductivity than $\text{Cs-}\beta\text{-ferrite}$ above 130°C , which is the melting point of CsTFSA (ca. 120°C), and demonstrated the very high Cs^+ ion conductivity of $3.4 \times 10^{-2} \text{ S cm}^{-1}$ at 250°C , which was 30 times that of $\text{Cs-}\beta\text{-ferrite}$.

References and Notes

- 1 R. D. Shannon, *Acta Crystallogr., Sect. A* **1976**, *32*, 751.
- 2 S. Ito, S. Nariki, K. Kozawa, T. Uchida, N. Yoneda, *Solid State Ionics* **1994**, *72*, 300.
- 3 E. I. Burmakin, S. S. Stroeve, G. Sh. Shekhtman, *Inorg. Mater.* **2009**, *45*, 80.
- 4 E. I. Burmakin, G. Sh. Shekhtman, *Russ. J. Electrochem.* **2009**, *45*, 564.
- 5 E. I. Burmakin, G. Sh. Shekhtman, *Russ. J. Electrochem.* **2009**, *45*, 1363.
- 6 Y. W. Kim, A. Oda, N. Imanaka, *Electrochem. Commun.* **2003**, *5*, 94.
- 7 N. Imanaka, Y. W. Kim, K. Ando, S. Tamura, *J. Mater. Sci.* **2005**, *40*, 3689.
- 8 N. Imanaka, I. Hasegawa, S. Tamura, *Sens. Lett.* **2006**, *4*, 340.
- 9 Supporting Information is available electronically on the CSJ-Journal Web site, <http://www.csj.jp/journals/chem-lett/index.html>.